Available online at www.sciencedirect.com

ScienceDirect

Energy Procedia 142 (2017) 1570–1576

Energy Procedia

www.elsevier.com/locate/procedia

9th International Conference on Applied Energy, ICAE2017, 21-24 August 2017, Cardiff, UK

Finite-rate chemistry modelling of non-conventional combustion regimes

Zhiyi Li[a], Alberto Cuoci[b], Amsini Sadiki[c], Alessandro Parente[a]*

[a]*Université Libre de Bruxelles, Aero-Thermo-Mechanics Department, Belgium*
[b]*Politecnico di Milano, Department of Chemistry, Materials, and Chemical Engineering, Italy*
[c]*Technische Universität Darmstadt, Institute of Energy and Powerplant technology, Germany*

Abstract

The present work deals with the numerical simulation of Adelaide Jet in Hot Co-flow burner under Moderate or Intense Low oxygen Dilution (MILD) conditions, using the Partially Stirred Reactor (PaSR) model for turbulence-chemistry interactions. The PaSR model assumes that reactions are confined in specific regions of the computational cells, whose mass fractions depend both on the mixing and the chemical time scales. Therefore, the appropriate choice of mixing and chemical time scales becomes crucial to ensure the predictivity of the numerical simulations. Results show that the most appropriate choice for the evaluation of the mixing time scale in MILD regime consists in using the geometric mean of the Kolmogorov and the integral mixing time, rather than Kolmogorov or integral scales. This is supported by the validation of the numerical results against experimental profiles of temperature, major and minor species mass fractions. Moreover, the identification of the key species in the oxidation process allows to determine a chemical time scale that improves the prediction of centerline and upstream temperature predictions, compared to the results obtained by including all species in the evaluation of the chemical scale.

Peer-review under responsibility of the scientific committee of the 9th International Conference on Applied Energy.

Keywords: MILD combustion; JHC burner; PaSR combustion model; mixing time scales; chemical time scales

1. Introduction

Recently, the reduction of fossil fuel availability and the increasing environmental concerns associated to their utilization in conventional systems have pushed the development of new combustion technologies that feature high fuel flexibility, increased efficiency and low pollution emissions. Among them, Moderate or Intense Low oxygen Dilution (MILD) combustion [1], has drawn increasing attention recently. MILD combustion is characterized by

* Corresponding author. Tel.: +3226502680; Mob: +32471360708.
E-mail address: Alessandro.Parente@ulb.ac.be

1876-6102
Peer-review under responsibility of the scientific committee of the 9th International Conference on Applied Energy.
10.1016/j.egypro.2017.12.608

elevated reactant temperature and low temperature increase [1], intensive reactant and product mixing as well as no audible or visible flame under ideal conditions. Moreover, MILD combustion delivers very low NOx and CO emissions, high efficiency and high fuel flexibility [2, 3].

MILD combustion technology has been extended to many industrial applications. It was first introduced in industrial furnaces for methane combustion [4] and then extensively investigated for other gaseous fuels like hydrogen [5] and ethanol [6]. Recently, Xing et al. [6] evaluated the possibility of using liquid bio-fuels, diesel and kerosene fuels for gas turbine applications. They concluded that flameless combustor appears to have potential to substitute the conventional gas turbine combustor. Furthermore, Adamczyk et al. [7] analyzed the potential of oxy-MILD combustion for large scale pulverized coal boilers. Results of the preliminary simulations showed the possibility of efficiency increase of more than 3%. The MILD combustion concept was even extended to hybrid solar thermal devices, which combine concentrated solar radiation with combustion. According to Chinnici et al. [8], the integration of MILD combustion in a hybrid solar receiver can lead to increased thermal performances with respect to conventional flames.

MILD combustion is still worthy of further investigations and attention, especially for the interaction between turbulence and chemistry. To this purpose, the Adelaide Jet in Hot Co-flow (JHC) burner [9] is considered in the present paper. The current study focuses on Reynolds Averaged Navier-Stokes (RANS) simulations in combination with Partially Stirred Reactor (PaSR) model for turbulence/chemistry interactions, using detailed chemistry. Different formulations for the mixing and chemical time scales that control the mean species reaction rates are evaluated. To assess the modelling choices, the simulated temperature, major and minor species mass fractions are compared with the experimental values.

2. Combustion model

2.1. Partially Stirred Reactor Model

In the PaSR model [10], the computational cell is split into two zones: one where reactions take place, and another only characterized by mixing. The final species concentration of the cell is determined from the mass exchange between the two zones driven by the turbulence. A conceptual drawing of the PaSR model is shown in Fig. 1,

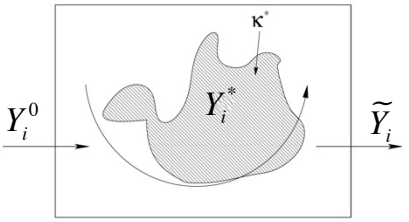

Fig. 1. Conceptual drawing of the PaSR model [11].

in which Y_i^0 is the initial species i mass fraction in the cell, $\widetilde{Y}_i$ is the final averaged i^{th} species mass fraction in the cell and Y_i^* is the i^{th} species mass fraction in the reaction zone. κ^* is the mass fraction of the reaction zone in the computational cell. The mean reaction rate $\overline{\omega}$ for species i in every computational cell can be expressed as:

$$\overline{\dot{\omega}_i} = \kappa^* \frac{\overline{\rho}(Y_i^* - \widetilde{Y}_i)}{\tau^*(1-\kappa^*)}, \tag{1}$$

where τ^* is the residence time of the fluid in the reaction zone and $\overline{\rho}$ is the mean density. The reaction zone can be considered as a Perfectly Stirred Reactor (PSR) or a Plug Flow Reactor (PFR). The mass fraction of the reaction zone κ^* is expressed with the following expression involving both the mixing and chemical time scales:

$$\kappa^* = \frac{\tau_c}{\tau_c + \tau_{mix}}. \tag{2}$$

In equation (2), the mixing time scale equals to the residence time in the reacting structures, $\tau^* = \tau_{mix}$.

2.2. Mixing and chemical time scales of PaSR model

Three different versions of the mixing time scale [11, 13, 14] in PaSR model are used in the current study. The first is based on the Kolmogorov mixing time scale.

$$\tau_{mix\_K} = \sqrt{\frac{\upsilon}{\varepsilon}} \tag{3}$$

In Eqn. 3, ν is the kinematic viscosity and ε is the turbulent kinetic energy dissipation rate. The second version consists in taking the integral time scale as characteristic scale:

$$\tau_{mix\_I} = C_{mix} \frac{k}{\varepsilon} \tag{4}$$

in which k is the turbulent kinetic energy and C_{mix} is a constant, which equals to 1.0 for high-Reynolds-number flow [15]. This choice might be justified in MILD regime considering that reactions are spread over a wide range of scales (i.e. distributed reaction regime) [12]. The last version is the geometric mean between the Kolmogorov time scale and the integral time scale [14], expressed as:

$$\tau_{mix\_M} = \sqrt{\tau_{mix\_K} \cdot \tau_{mix\_I}} \tag{5}$$

The chemical time scale in the PaSR model is estimated by evaluating, for each cell, the rate of change of the species within the chemical mechanism, and focusing on the ones controlling the main oxidation process. The chemical time scale of a single species is estimated by calculating the product of the mass fraction and the formation rate of each species [14]. In the present paper, the evaluations of the chemical time scale are based on the full KEE mechanism species and the key species which represent a subset of the KEE mechanism (CH_3, H_2O_2, CO_2, HCO, CH_2O, O, H, HO_2, CH and O_2) [16].

3. Experimental Basis and Numerical Settings

3.1. Jet in Hot Co-flow burner

The Adelaide Jet in Hot Co-flow burner has a central jet with the inner diameter of 4.25 mm. An equimolar mixture of CH_4 and H_2 is provided as the central jet fuel. There is an annulus tube within which an internal burner is mounted to provide hot products. The hot products are mixed with N_2 and O_2, therefore the mass fraction of O_2 can be controlled to different levels. In the current scope, the oxygen mass fraction of 3% in the hot co-flow is investigated. The annulus tube has the inner diameter of 82 mm. Moreover, the burner is mounted on a wind tunnel with the cross section of 254 mm×254 mm. The gas velocity and temperature of the central jet, annulus and the wind tunnel can be found in Table 1. The central jet fluid has a Reynolds number of 10,000. In Fig. 2, a 2D schematic drawing of the studied burner can be found. According to the experimental measurement [9], the mean and root-mean-square values of the temperature and species mass fractions are available on the centerline and axial positions of 30/60/120/200 mm.

Table 1. Physical properties of the Adelaide JHC jet.

Locations	Temperature	Velocity
Central jet	294 K	58.74 m/s
Annulus	1300 K	3.2 m/s
Tunnel	294 K	3.3 m/s

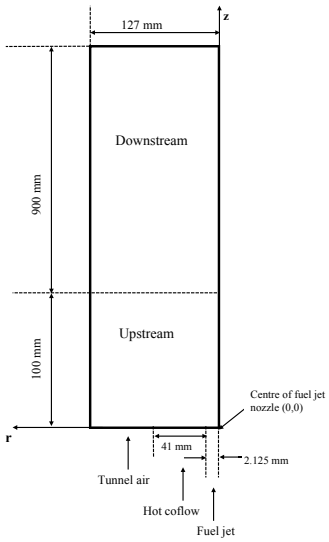

Fig. 2. 2D schematic drawing of the Adelaide JHC burner (adapted from Ferrarotti et al. [17])

3.2. Numerical Settings

An axi-symmetric 2D mesh with 35000 cells is constructed for the simulation. The computational domain starts from the exit of the burner and extends on axial direction until 1000 mm downstream. The boundary conditions are set as in Table 2.

Table 2. Boundary condition settings for the simulation of the Adelaide JHC burner.

Boundaries	Temperature (K)	Velocity (m/s)	CH4 mass fraction (-)	H2 mass fraction (-)	O2 mass fraction (-)
Inlet fuel	305	58.74	0.888	0.112	0
Inlet coflow	1300	3.2	0	0	0.03
Inlet air	294	3.3	0	0	0.232

A transient simulation with the OpenFOAM® based solver pasrPimpleSMOKE [18] is used for the current simulation. In the solver, multi-component molecular diffusion is implemented to account for the high molecular diffusion coefficient of H_2. The turbulent Schmidt and Prandtl numbers are taken as 0.7 and 0.85, respectively. The Standard k-epsilon model constant $C_{1\epsilon}$ is adjusted to 1.60. The KEE [19] mechanism with 17 species and 58 reactions is used for the detailed chemistry approach.

4. Results and Discussion

In this section, the mean values of temperature, CO_2 mass fraction and OH mass fraction predictions using different mixing and chemical time scale definitions will be presented and compared with the experimental data available at 30/60/120 mm downstream of the burner exit and along the centerline.

Fig. 3 shows the comparison between the experimental mean temperature profiles and the simulation results obtained with three different mixing time scales (a) and two different chemical time scales (b). In Fig. 3(a), tauK indicates the Kolmogorov mixing time scale, tauI means the integral mixing time scale and tauMean is the geometric mean of the above two. The results in Fig. 3(a) are obtained using all the species in the KEE mechanism to compute the chemical time scale. In Fig. 3(b), tauI-all shows the results obtained using all species in the mechanism for chemical time scale, while tauI-important indicates the chemical time scale calculated using the key species only. The same nomenclature is used in Fig. 4 and Fig.5.

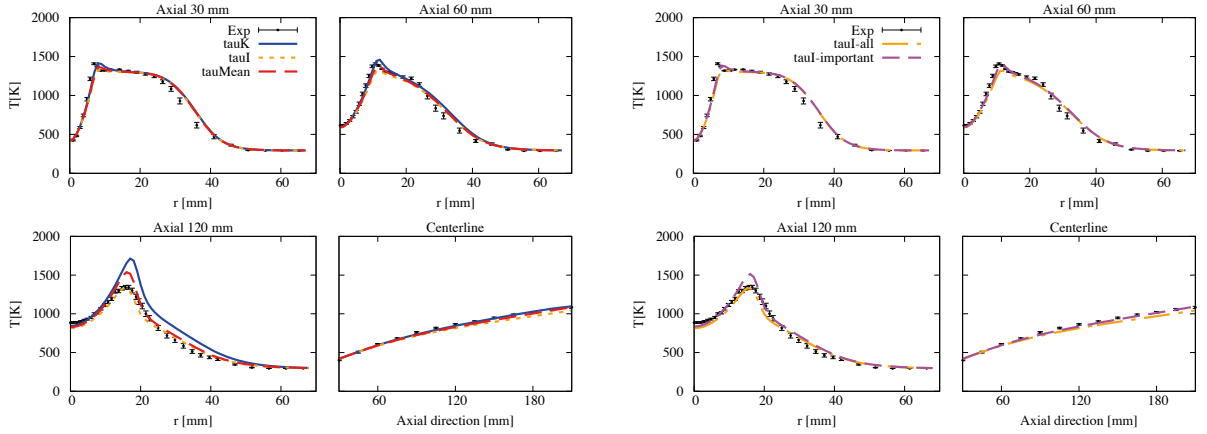

(a) Different mixing time scales (b) Different chemical time scales

Fig. 3. Mean temperature profiles of PaSR model with different mixing time scales (a) and different chemical time scales (b).

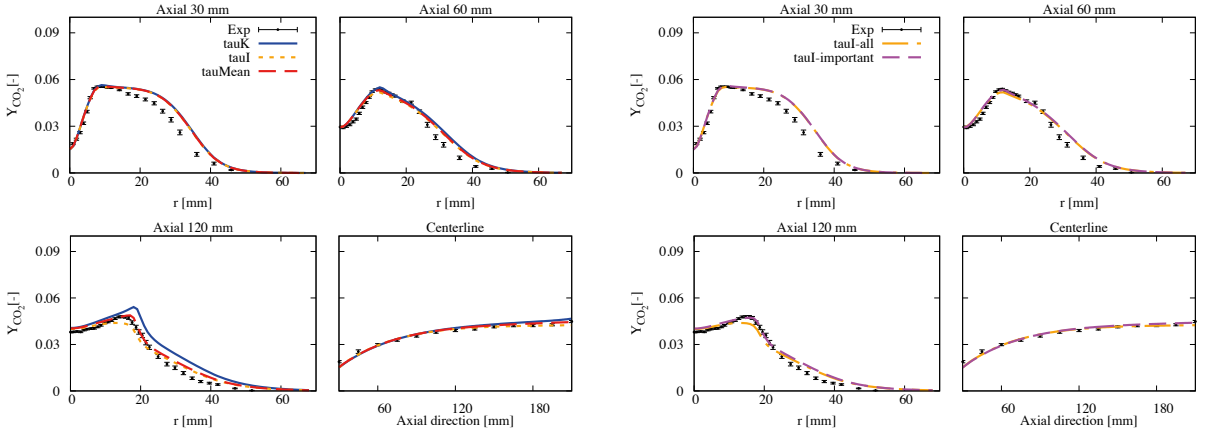

(a) Different mixing time scales (b) Different chemical time scales

Fig. 4. Mean CO2 mass fraction profiles of PaSR model with different mixing time scales (a) and different chemical time scales (b).

From Fig. 3(a), one can observe that the Kolmogorov mixing time scale gives slight over-prediction of temperature on the centerline and 60 mm axial position. The over-prediction is even more significant at 120 mm axial position and this also affects the prediction of the OH mass fraction profile in Fig. 5. Using the integral mixing time scale, in Fig. 3(a), the temperature profiles are under-predicted at 30 and 60 mm downstream of the burner, and along the centerline. On the other hand, the temperature peak at 120 mm axial location is well predicted. However, the use of the integral mixing time scale does not improve the prediction of CO_2 and OH mass fractions on 120mm axial location, in Fig. 4(a) and Fig. 5. When the geometric mean of the two scales is applied in the simulation, the 30 mm 60mm and centerline temperature profiles match well with the experimental ones. A slight over-prediction of the temperature profile at 120 mm axial location can be observed, while the CO_2 and OH mass fraction profiles are well captured. Fig. 3(b) and Fig. 4(b) compare the results obtained using two sets of species for the evaluation of the chemical scales. Using the chemical time scale based on the key species, it is possible to correct the generalized under-prediction observed using all the species in the mechanism.

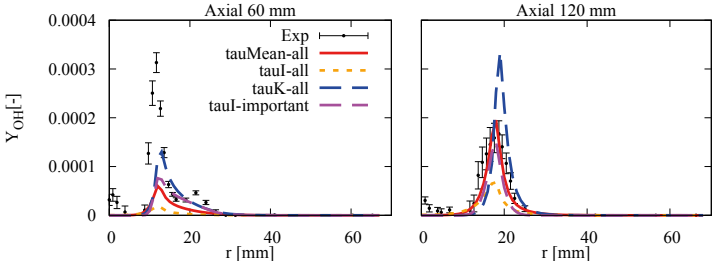

Fig. 5. Mean OH mass fraction profiles of PaSR model with different mixing time scales and different chemical time scales.

5. Conclusion

In this paper, the Adelaide JHC burner under MILD combustion condition is investigated using RANS and the PaSR combustion model for turbulence-chemistry interactions. The main conclusions can be summarized as follows:

- The Kolmogorov mixing time scale results in over-prediction of temperature on most sampled positions, while the integral mixing time scale gives under-prediction.
- The geometric mean of the Kolmogorov and integral mixing time scales gives the best simulation result regarding mean temperature, CO_2 and OH mass fraction profiles.
- Using the *key* species to estimate the chemical time scale allows to correct the under-prediction obtained using all the species in the kinetic mechanisms to compute the characteristic chemical time scale.

Furthermore, the improvement of combustion modelling in MILD combustion is crucial to the simulation of industrial applications featuring new combustion technologies designed to burn multiple fuels in non-conventional combustion regimes.

Acknowledgements

This project has received funding from the European Union's Horizon 2020 research and innovation program under the Marie Sklodowska-Curie grant agreement No. 643134 and the European Research Council (ERC) grant agreement No. 714605. The last Author would like to acknowledge the support of Fédération Wallonie-Bruxelles, via "Les Actions de Recherche Concertée (ARC)" call for 2014-2019, to support fundamental research.

References

[1] J. A. Wünning, J. G. Wünning, Flameless oxidation to reduce thermal NO-formation, Progress in Energy and Combustion Science 23, 81-94, 1997.
[2] A. Cavaliere, M. de Joannon, MILD combustion, Progress in Energy and Combustion Science 30, 329-366, 2004.
[3] P. R. Medwell, B. B. Dally, Effect of fuel composition on jet flames in a heated and diluted oxidant stream, Combustion and Flame 159, 3138-3145, 2012.
[4] C. Galletti, A. Parente, L. Tognotti, Numerical and experimental investigation of a mild combustion burner, Combustion and Flame 151, 649-664, 2007.
[5] A. Parente, C. Galletti, L. Tognotti, Effect of the combustion model and kinetic mechanism on the MILD combustion in an industrial burner fed with hydrogen enriched fuels, International Journal of Hydrogen Energy 33 (24), 7553-7564.
[6] F. Xing, A. Kumar, Y. Huang, S. Chan, C. Ruan, S. Gu, X. Fan, Flameless combustion with liquid fuel: A review focusing on fundamentals and gas turbine application, Applied Energy 193, 28-51, 2017.
[7] W. P. Adamczyk, R. A. Bialecki, M. Ditaranto, P. Gladysz, N. E. L. Haugen, A. Katelbach-Wozniak, A. Klimanek, S. Sladek, A. Szlek, G. Wecel, CFD modelling and thermodynamic analysis of a concept of a MILD-OXYcombustion large scale pulverized coal boiler, Energy xxx, 1-11, 2017.
[8] A. Chinnici, Z. F. Tian, J. H. Lim, G. J. Nathan, B. B. Dally, Comparison of system performance in a hybrid solar receiver combustor operating with MILD and conventional combustion. Part II: Effect of the combustion mode, Solar Energy 147, 478-488, 2017.
[9] B. B. Dally, A. N. Karpetis, R. S. Barlow, Structure of turbulent non-premixed jet flames in a diluted hot co-flow, Proceedings of the Combustion Institute 29, 1147-1154, 2002.
[10] V. I. Golovitchev, J. Chomiak, Numerical modelling of high temperature air "flameless" combustion, Chalmers University of Technology,

Göteborg, 41296 Sweden.
[11] P. A. N. Nordin, Complex chemistry modelling of diesel spray combustion, Chalmers University of Technology, Göteborg, 41296 Sweden.
[12] A. Parente, M. R. Malik, F. Contino, A. Cuoci, B. B. Dally, Extension of the Eddy Dissipation Concept for turbulence/chemistry interactions to MILD combustion, Fuel 163, 98-111, 2016.
[13] L. Kjäldman, A. Brink, M. Hupa, Micro mixing time in the Eddy Dissipation Concept, Combustion Science and Technology, 154, 207-227, 2007.
[14] J. Chomiak, A. Karlsson, Flame lift-off in diesel sprays, Twenty-Sixth Symposium (International) on Combustion/The Combustion Institute, 2557-2564, 1996.
[15] Y. Liu, R. O. Fox, CFD predictions for chemical processing in a confined impinging-jets reactor, American Institute of Chemical Engineers Journal, 52 (2), 2006.
[16] B. J. Isaac, A. Parente, C. Galletti, J. N. Thornock, P. J. Smith, L. Tognotti, A novel methodology for chemical time scale evaluation with detailed chemical reaction kinetics, 27(4), 2255-2265, 2013.
[17] M. Ferrarotti, C. Galletti, A. Parent, L. Tognotti, Development of reduced NOx models for flameless combustion, 18th IFRF members conference, 2015.
[18] URL: https://github.com/acuoci/edcSMOKE
[19] R. W. Bilger, S. H. Starner, R. J. KEE, On reduced mechanisms for methane-air combustion in non-premixed flames, Combustion and Flame 80 (2), 135-149, 1990.